[3] Зубова. С. П., Раецкая Е. В., Jle Хай Чунг. О полиномиальных решениях линейной стационарной системы управления. Автоматика и Телемеханика, №11, 2008. с. 41 - 47.

[4] Зубова СП, Чан Тхань Туан . Построение быстро убывающего решения неоднородной системы при наличии контрольных точек и условий на управление . Автоматика и телемеханика. 2010. № 11. С. 29-37.

[5] Каган В.Ф, Основание теории определителей. Одесса.: Госуд. Из-во Украины,1922.521с.

[6] Раецкая Е. В. Условная управляемость и наблюдаемость линейных систем: Дисс. канд. физ. мат. наук. Воронеж, 2004.

[7] Ailon A., Langholz G, More on the controllability of linear time-invariant systems. Int. J. Contr. 1986. Volume 44 . P. 1161 - 1176.

[8] Ailon A., Polynomial controllability in linear time-invariant systems: some further results and applications to optimal control . 15th Triennial Word Congress, Barcelona,Spain.P.449-454.

[9] Lena Scholz, Control theory of descriptor systems lecture notes. TU Berlin (WS2014/15).2015.

[10] S. P. Zubova, Le Hai Trung, Construction of polynomial controls for linear stationary system with control points and additional constrains. Automation and Remote Control. Volume 71, Number 5. Pages: 971-975. 2010.

LONG-TERM TRENDS IN THE UPPER AND LOWER IONOSPHERE

DOI: 10.31618/ESU.2413-9335.2019.4.65.278

Gordiyenko G. I.
Institute of Ionosphere, National Center for Space Research and Technology, PhD (Geophysics) Leading Researcher, Almaty 050020, Kazakhstan
Yakovets A. F.
Institute of Ionosphere, National Center for Space Research and Technology, PhD (Geophysics) Leading Researcher, Almaty 050020, Kazakhstan
Litvinov Yu. G.
Institute of Ionosphere, National Center for Space Research and Technology, PhD (Geophysics) Leading Researcher, Almaty 050020, Kazakhstan

ABSTRACT

Long-term variability of foF2 and fmin observed at the midlatitude Alma-Ata [43.25ºN, 76.92ºE] are analyzed for the period 1957-2017.

The geomagnetic (Ap) indexes, the near-noon, near-midnight, daily averaged foF2, and near-noon fmin variations are found to be in strong dependence from the solar activity; all of them show a dominant pattern of variation with a period of ~34-36 years and linear negative trend. The correlation coefficient between the foF2 and F10.7 long-term variations is very high, up to 0. 99 that permit us to believe that the solar activity can be considered to be the main driver for the long-term variations in the ionospheric F2-region.

The long-term course of fmin is similar to those found in F10.7, Ap, and foF2, i.e. the periodicity of 34-36 years is also evident in the fmin variations. However, in contrast to the F2-layer parameters, the fmin variation clear demonstrates an upward (positive) linear trend that is opposite in sign to the trend found in the F10.7. This means relatively high sensitivity of the fmin values to the solar activity changes and significant influence of other trend drivers on them, one of which is the possible impact of anthropogenic factors on the state of the lower ionosphere.

Keywords: Midlatitude ionosphere; upper and lower ionosphere; ionosonde data, long-term trends.

Introduction

In ninetieth, an effect on HF/VHF radio propagation due to the "greenhouse cooling" associated with lowering of the F2-layer was predicted [1-3]. Using the NCAR Thermosphere/Ionosphere General Circulation Model the authors predicted that "the thermospheric temperature will be lowered by 30-40K and the air density at heights of 200-3000 km will be reduced by 20-40%, thus increasing the orbital lifetimes of satellites. The height of the ionospheric F2-layer peak will drop on average by about 15 km, with some effect on radio propagation, though the F2-layer critical frequency will hardly be affected". A lot of investigations have been carried out to test this prediction using ionosonde observations at different stations. The long-term variations in the ionosphere parameters have been the subject of a number of observational [4-18] and modelling [19-21] studies as reviewed in [22-30]. Different values for trend in foF2 have been obtained in the studies, from -0.00022 [9] to -(0.01-0.02) MHz/year [31].The most probable causes of such discrepancies are: different length of the data series for which the trends are determined, different methods used to extract long-term trends from observations, different time period selections for the foF2 trend analyses (different seasons, different phases of cycles in solar activity). For example, to analyze the foF2 trends it is necessary to exclude as much as possible the dependence of foF2 data on solar (and geomagnetic) activity effects, it means a special model must be used. Regression dependence between foF2 and solar and geomagnetic indexes is used as a model. Then, relative deviations of the observed foF2 values from the model ($\delta foF2 = (foF2_{obs} - foF2_{mod})/foF2_{mod}$ (i.e. [18]) or $\delta foF2 = (foF2_{obs} - foF2_{mod})/foF2_{obs}$ (i.e. [15]) or absolute values ($\delta foF2 = foF2obs - foF2mod$ (i.e. Bremer [10, 32]) are analyzed in the trend study. The first two regression dependences are practiced to combine different months and obtain an annual mean

δfoF2 that is used in the analyses, with the final method being based on the 11-year running mean δfoF2 values.

In our previous work [33] we investigated the long-term variations in the near-noon (10-14 LT) critical frequency of the ionospheric F2-layer (foF2) measured at the mid-latitude station Alma-Ata [43.25°N, 76.92°E] over the period from 1957 to 2012. The absolute deviations (ΔfoF2) of monthly median foF2 values from the model foF2 data smoothed by the 11-year (132 months) running mean method were used in that trend study. The second-order polynomial dependence between monthly median foF2 values and F10.7 was assumed to calculate the model foF2 values. It was also shown that the geomagnetic activity (described by Ap index) is strongly linked to the solar cycle phase, and in that study, we did not exclude variation in foF2 related to geomagnetic activity. As a result, it was shown that the critical frequency is significantly correlated with the solar activity demonstrating the 11-year solar cycle, a 30-32-year variation, and a stable tendency for the decrease (a negative foF2 trend) correlating with the negative trend in variation of solar radio flux F10.7. The magnitude of the trend was found to be -0.0038 MHz/year for the deviations $\Delta foF2_{132}$ that is in the frame of the trends found in the studies mentioned above. A dominant influence of the Sun on the ionosphere was proposed as the main reason for the found foF2 trend, that assumes an existence of cyclic variations of solar activity with a period of T>55 years.

The purpose of this paper is to provide further analyses of the F2-layer variations and to study long-term trends (a long-term linear change) in the near-noon, near-midnight and daily averaged critical frequencies F2-layer critical frequencies foF2 measured at the Alma-Ata station in more extended time period, from 1957 to 2017 including the period of very deep minimum of solar activity observed in 2008-2009. In addition to the F2-layer parameters the minimum frequency of reflection (fmin) is also used as a climatic characteristic of the upper atmosphere/low ionosphere (D region) to do the trend analysis in the ionospheric absorption.

Data and methods used

For the present trend analysis, monthly median foF2 and fmin values routinely measured at Alma-Ata station [43.25^0N, 76.92^0E] have been used. The arithmetic means of the foF2 values at the near-noon (10-14LT), near-midnight (23-01LT) hours, and daily means foF2 are calculated for the analyses; the fmin values are taken only for near-noon hours: $foF2_{10\text{-}14}$, $foF2_{23\text{-}01}$, $foF2_{d.av.}$, and $fmin_{11\text{-}13}$ correspondingly. The monthly mean solar flux F10.7 and geomagnetic index Ap are also used as the indices for solar and geomagnetic activity (available at http://www.swpc.noaa.gov/) to illustrate their long-term varioations. The ionospheric data cover about six solar cycles (during 1957-2017); solar data are available from 1947, geomagnetic data – from 1932.

As an example, median mean values of $foF2_{10\text{-}14}$, $foF2_{23\text{-}01}$, and $foF2_{d.av.}$ together with the corresponding data of solar and geomagnetic activity are shown in Figure 1a-e. The dots represent observed data, and the thick lines show the fitting of the observed data with 27-day running mean values illustrating the dominant 11-year cyclic pattern. It should be also noted that the statistical processing of the foF2 data series requires their continuity that is not always possible. Since the observational time period is so long (60 years), there are some observational gaps in the ionospheric data sets because of different reasons such those: median estimations were subject of significant uncertainties, ionosonde repairs, preventive diagnostics, and other technical problems. The regression dependences between the selected ionospheric parameters and F10.7 (Figure 1f-h) have been analyzed to define the missing data. Thick lines represent the linear regression line for these data; dashed lines correspond to the polynomial functions of the second degree that best fit the given F2-layer parameters as function of F10.7 ($R^2_{polinomial} > R^2_{linear}$). A higher-order (cubic) regression does not provide any significant improvement to the fit: R^2 = 0.81856 (r = 0.91), 0.421752 (r = 0.65), 0.800255 (r = 0.89) for a second-order regression the critical frequencies versus F10.7, R^2 = 0.818617, 0.422152, 0.80028 for a third-order regression, where R^2 is the coefficients of determination that provides a measure of how well the least-square curve fits the observational data, r is the correlation coefficient. Assuming the second-order polynomial dependence with F10.7, the missing foF2 values have been defined from the regression equations to fill available gaps in the data sets.

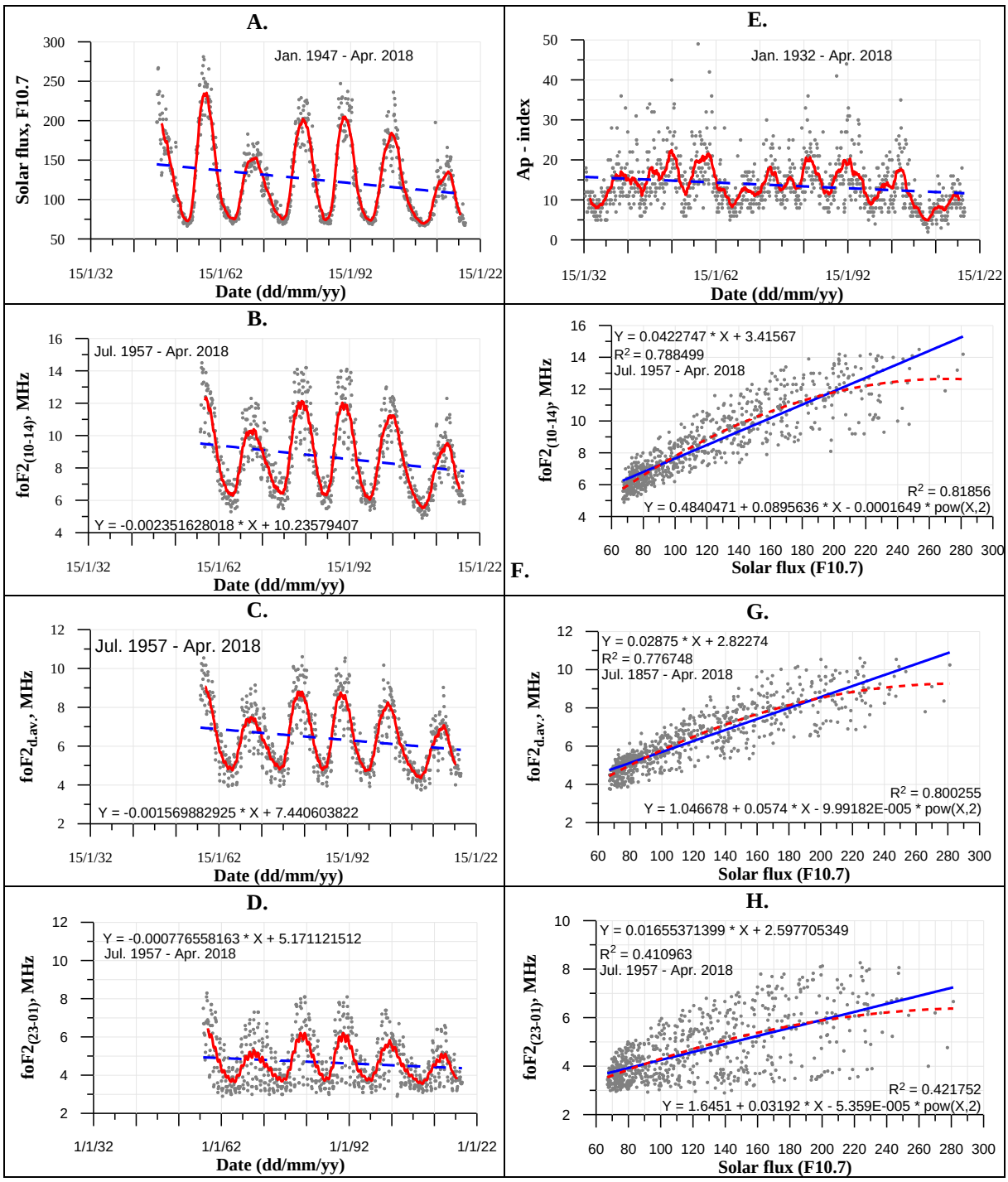

Figure 1. The long-term variations of the near-noon (b), daily mean (c) and near-midnight (d) monthly median foF2 values in Alma-Ata [43.250N, 76.920E] in 1958-2017 together with the corresponding variation of solar flux F10.7 (a) and Ap index (e); solid dots - measured data, thick lines show the fitting of the data with 27-day running mean values, dashed lines – linear fits. Monthly median near-noon (f), daily mean (g) near-midnight (h) and foF2 values versus monthly mean F10.7; thick lines represent the linear regression line for these data, dashed lines correspond to the polynomial functions of the second degree.

Data related to the D region are much more limited than those related to the F region. This is due to the fact that reflections from layer D in vertical incidence are rarely obtained due to the large absorption caused by the high frequency of collisions of ions with the neutral neutrals of air at given heights. The absorption effect appears on the ionogram as an increase in the minimum frequency of reflections fmin [34]. It should be noted, the minimum frequency of reflection depends, apart from the absorption of radio waves in the ionosphere, on sensitivity of the recording system of the ionosonde, on levels of natural and industrial noise. Hence, the complex dependence of the fmin on the technical characteristics of the ionosonde makes it impossible to use this ionosphere parameter to measure the absolute values of the absorption of radio waves. However, as a qualitative characteristic, as an indicator of absorption of radio waves, the value of fmin is widely used ([35-36] and references therein).

Trends in the F and D regions. Results and Discussion.

In this Section, we present some results of the trend study for ionospheric parameters derived from ionosonde measurements for the two ionospheric regions, for the F and D layers.

Trends in the F region. As stated above, in the study presented here monthly median values of the following ionosonde parameters of the F-region are used: the F2-layer near-noon (10-14LT), near-midnight (23-01LT), and daily means critical frequencies values foF2. The $foF2_{10\text{-}14}$, $foF2_{23\text{-}01}$, and $foF2_{d.av.}$ values of the station Alma-Ata have been presented in Figure 1a-e together with solar flux F10.7 and Ap index. Two things are evident in the figure, firstly the variations of all parameters are strictly modulated by cyclic ~ 11-year variations of solar activity and secondly the foF2 data are much scattered relative to the smoothed lines that can be attributed to various sources other than solar activity, including planetary waves and seasonal variations. As an example, the great part of seasonal variations is evident in Figure 1e where large deviations of the $foF2_{23\text{-}01}$ values from the smoothed line is caused by the fact that summer nighttime foF2 values are much higher than winter ones. Since this intraseasonal variability has to be taken into consideration in the trend analysis, annual running averages of the parameters considered were calculated. Figure 2a-e demonstrates temporal variations of the calculated annual averages (denoted by symbol *) of the $F10.7^*$, Ap^* indexes, and the F2-layer parameters ($foF2^*_{10\text{-}14}$, $foF2^*_{23\text{-}01}$, and $foF2^*_{d.av.}$) for the whole period of observations; variations of the annual averages of $foF2^*_{10\text{-}14}$, $foF2^*_{23\text{-}01}$, and $foF2^*_{d.av}$ with $F10.7^*$ are presented in Figure 2f-h. The main feature of the variations is their similarity (Figure 2a-e) and close connection between the ionospheric parameters and solar activity (Figure 2f-h). The coefficients of determination R^2 (the coefficients R^2 and derived regression equations are shown in the figure fields) are found to be very high, from 0.97 to 0.99, it means that from 97% to 99% of the annual foF2 variations can be explained by their relationship with the 11-year cycle of solar activity.

As we did in our previous work [33], the 11-year (132 months) running mean values of the annual averages of the ionospheric parameters ($foF2^*_{10\text{-}14}(132)$, $foF2^*_{23\text{-}01}(132)$, and $foF2^*_{d.av}(132)$.) were calculated over the entire data sets according to the method set out by Mikhailov [12] to obtain an independent picture of long-term trends in the upper ionosphere; the 11-year smoothing technique was also applied to the F10.7 and Ap data sets ($F10.7^*(132)$, $Ap^*(132)$); Figure 3 presents these calculated values. Figure 3a-e demonstrates that ionospheric parameters, solar and geomagnetic indices tend to behave similarly. The dots denote the observed data; thick lines represent the polynomial functions that best fit the given parameters as function of time.

Note, that geomagnetic activity is strongly controlled by the solar activity, both shows a dominant pattern of variations with a period of ~34-36 years that are also reflected in all ionospheric parameters considered. This period slightly differs from our earlier finding [33] where the period was estimated to be in a range of 30-32 years. The extended data sets used in the study reveal the period more clearly. Dashed lines in Figure 3a-e represent the negative linear long-term trends in Ap, F10.7, and in the F2-layer parameters as well. Note, that the negative trends, the lowering in the critical frequencies, can be also seen in Fig. 1 and Fig. 2. To interpretation of the period of 34-36 years it should be mentioned that the period of 31-33 years has been found in all the solar terrestrial parameters ([37, 38, 39] and references there in). A possibility is that this period of 31-33 years is the solar origin of the 35-year Bruchner climatic periodicity ([40, 41] and references there in).

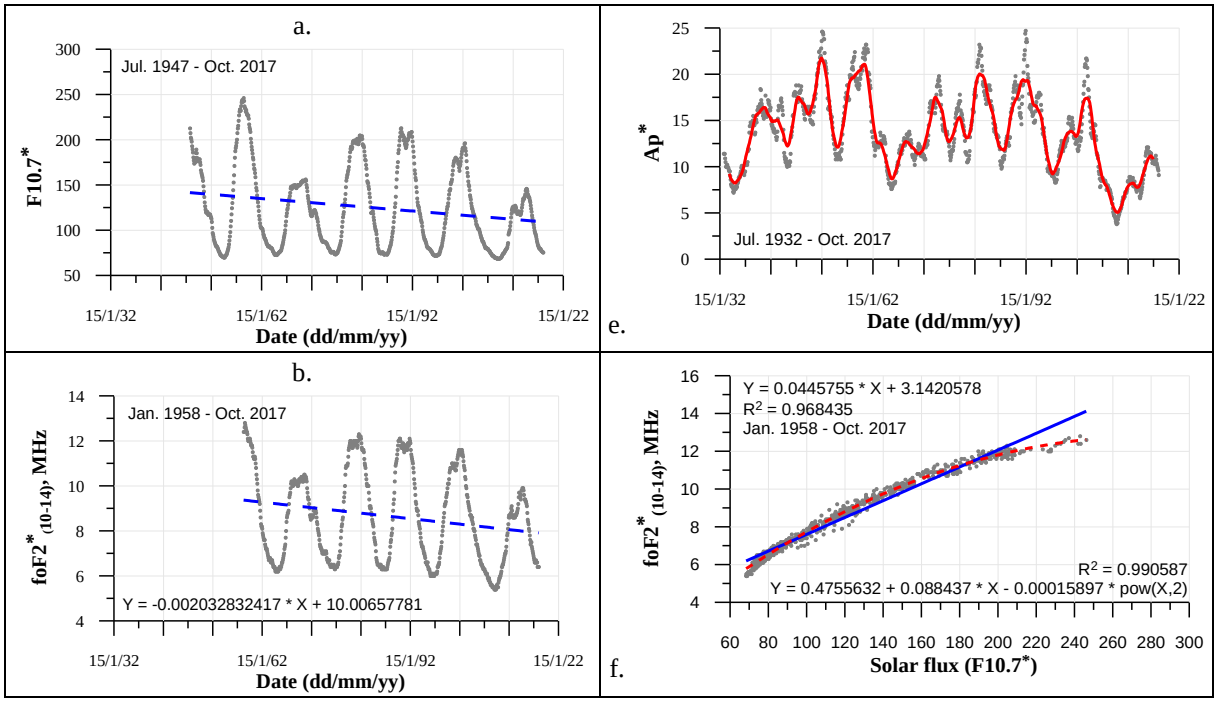

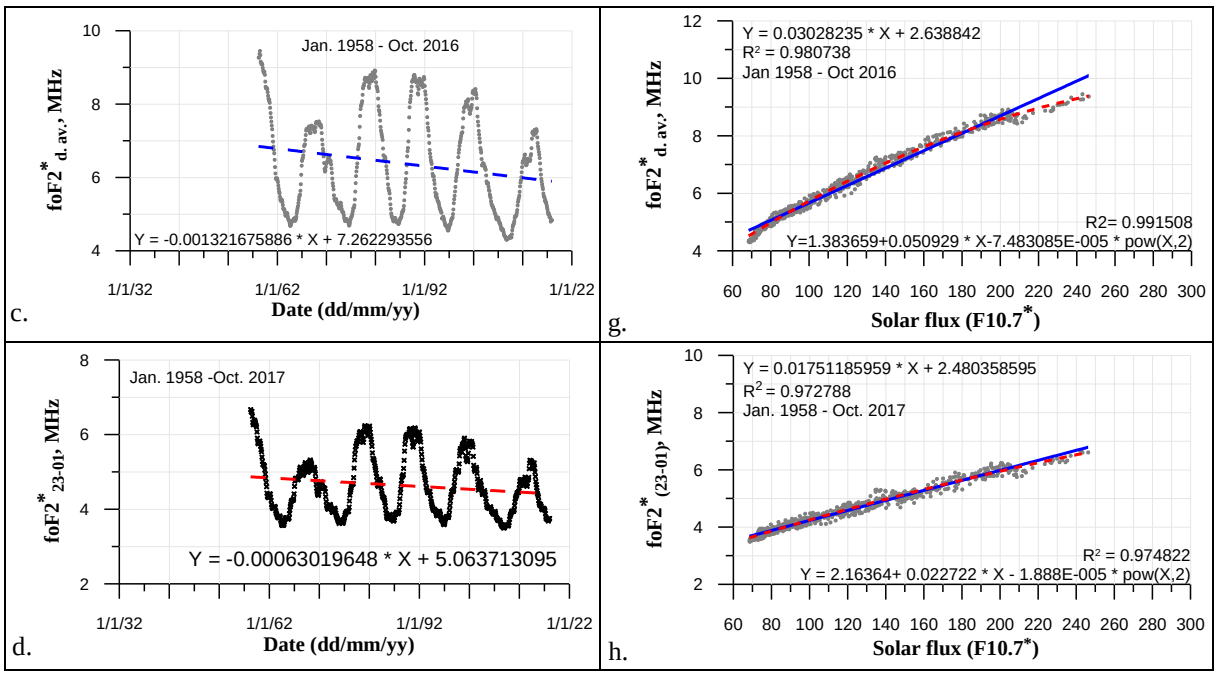

Figure 2. As the Figure 1but for the annual averages of the F10.7, Ap, and foF2 values.

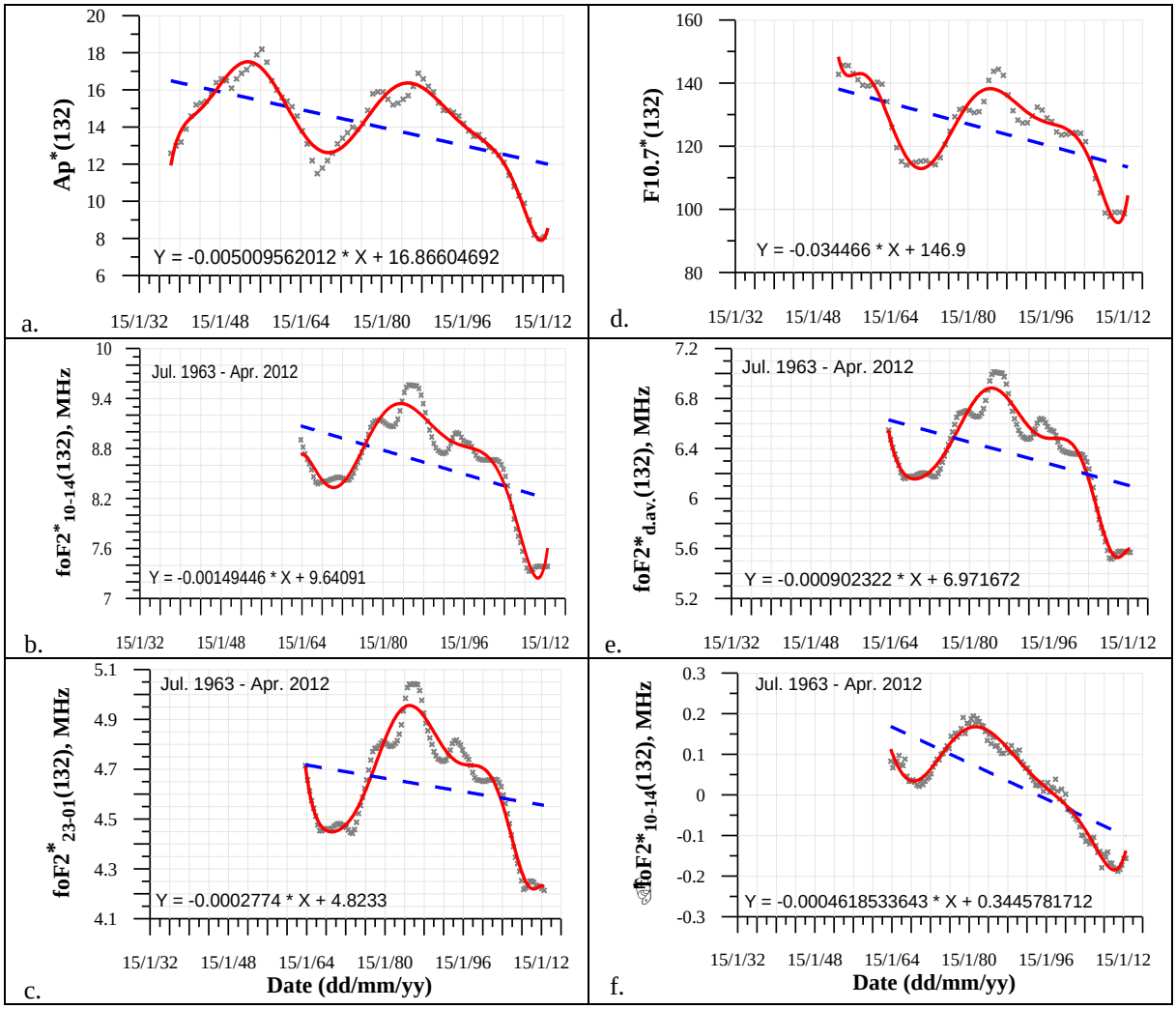

Figure 3. The 132-month smoothed values of the annual averages of the ionospheric F2-layer parameters, F10.7 and Ap.

Additionally (as an example), assuming the second-order polynomial dependence between foF2*$_{10-14}$ and F10.7* (see Fig. 2b) the effect in foF2*$_{10-14}$ related to the solar activity was removed to define the

deviation $\Delta foF2^*_{10\text{-}14}$.Then, the residual $\Delta foF2^*_{10\text{-}14}$ were smoothed using the 11-year running mean smoothing. The $\Delta foF2^*_{10\text{-}14}(132)$ long-term variations and $\Delta foF2^*_{10\text{-}14}(132)$ linear trend are shown in Fig. 3f. One can see that the $\Delta foF2^*_{10\text{-}14}(132)$ shows variation similar to those seen in Figs. 3a-e. Long-term trends in different ionospheric characteristics are shown in Table 1.

Table 1

THE EXPERIMENTAL TRENDS DERIVED FROM TREND ANALYSIS OF DIFFERENT F2-LAYER CHARACTERISTICS OBSERVED AT THE ALMA-ATA STATION [43.25^{0}N, 76.92^{0}E].

#	Parameter	Trend, MHz/Year	Parameter	Trend, MHz/Year	Parameter	Trend, MHz/Year
1	$foF2_{10\text{-}14}$(med)	-0.02822	$foF2^*_{10\text{-}14}$	-0.02439	$foF2^*_{10\text{-}14}$ (132)	-0.01758
2	$foF2_{d.av}$ (med)	-0.01884	$foF2^*_{d.av}$	-0.01586	$foF2^*_{d.av}$ (132)	-0.01077
3	$foF2_{23\text{-}01}$ (med)	-0.00932	$foF2^*_{23\text{-}01}$	-0.00756	$foF2^*_{23\text{-}01}$ (132)	-0.00364
4	-	-	-	-	$\Delta foF2^*_{10\text{-}14}$ (132)	-0.00554

The generally negative trends and the same order of magnitude of the trends in all foF2 characteristics are found (Table 1, lines 1-3) independently of the fact whether the solar activity effects are excluded or not. One exception, the trend in the near-noon $\Delta foF2^*_{10\text{-}14}(132)$ values is a third of the near-noon $foF2^*_{10\text{-}14}(132)$ trend, about -0.00554 MHz/year that is close to the trend obtained in our previous study [33], -0.0038 MHZ/year.

Figure 4 (left panel) illustrates the regression dependence of $foF2^*_{10\text{-}14}$, $foF2^*_{23\text{-}01}$, and $foF2^*_{d.av.}$ on F10.7*(132) for the period 1963-2012 (the 11-year smoothing technique that was applied to the foF2* data sets reduced the available period for study to between 1963 and 2012), the solid lines show the linear approximations of the points. The coefficients of determination (R^2) are equal to 0.96, 0.98, and 0.99 for near-noon, daily averaged and near-midnight data correspondingly. However, a combination of two groups of points is evident in Fig.4 that assumes some different dependence between the parameters on different phases of the 34-36 years cycle (the period 1972-1984, and 1984-2008), when the foF2*(132) values increase to their maximum and then decrease to their minimum values. Examples of the regression dependences between foF2*(132) and F10.7*(132) for the two time periods are shown in Figure 4 (two right panels). It is distinctly seen in both cases that 99% of the variations in the ionospheric parameters can be explained by linear dependence between them and solar activity, R^2=0.992-0.999. So, the solar activity can be considered to be the main driver for the long-term variations in the ionospheric F2-region.

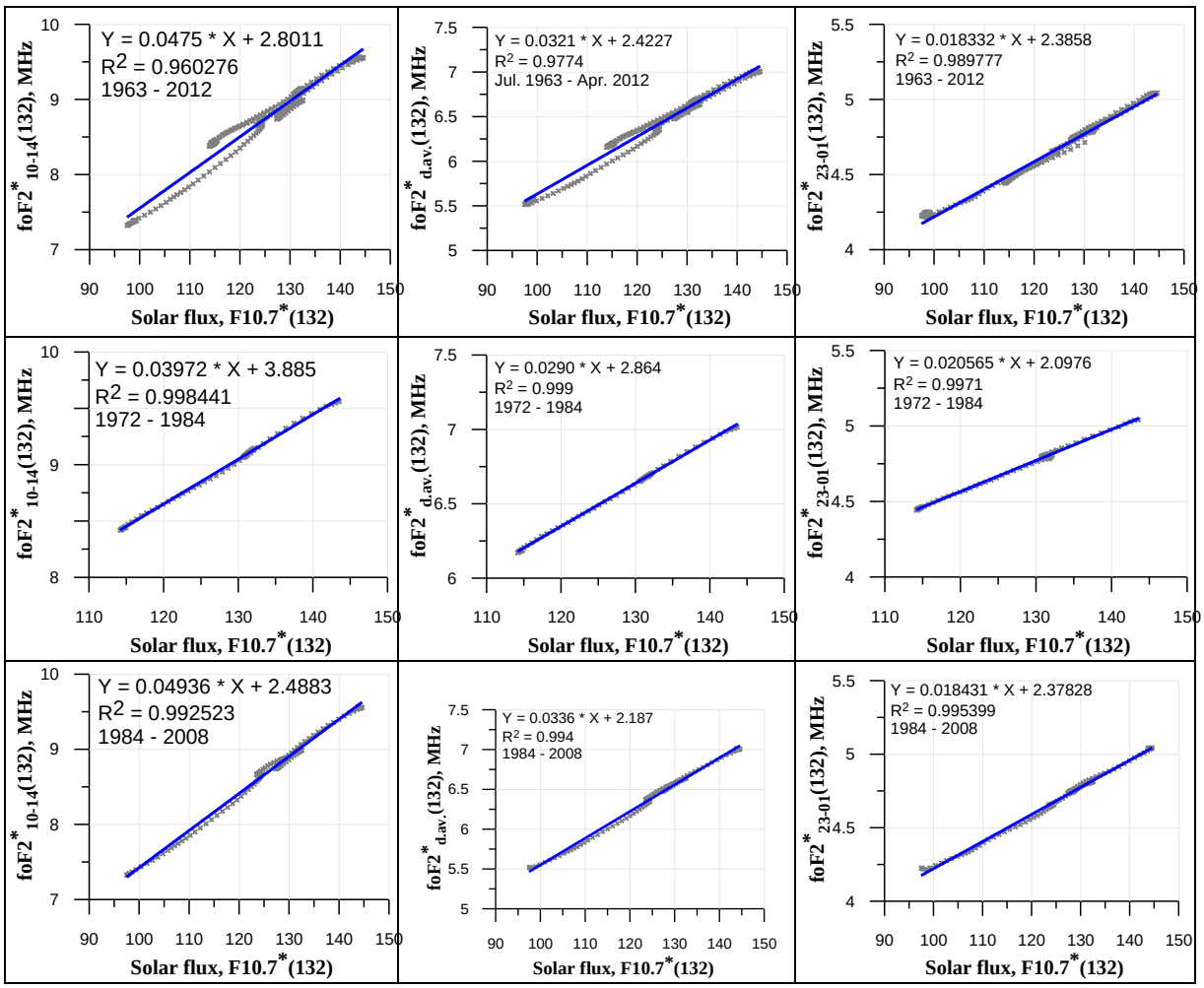

Figure 4. The regression dependence of the 132-month smoothed foF2$_{10\text{-}14}$, foF2*$_{23\text{-}01}$, and foF2*$_{d.av.}$ values on F10.7*(132) for the whole measuring interval (1963-2012, upper panel), and for the periods of increasing (1972-1984, middle panel) and decreasing (1984-2008, bottom panel) of the solar activity.*

Trends in the D region. A similar analysis, as that carried out for foF2 in the years 1957-2017, has been carried out for all the years in the fmin data observed at the station Alma-Ata [43.25ºN, 76.92ºE]. As it has been already mentioned in Section 1, the ionospheric parameter fmin is used as a qualitative characteristic of the ionospheric absorption in the D-region, and our interest is understand "is there any trend in the fmin data, and what its sign?" For this purpose, we use the monthly median fmin values for the near-noon interval of local time (11-13 LT) averaging the data over three hours, from 11:00 LT to 13:00 LT. F10.7 dependence of the measured fmin for the period is shown in Figure 5a where each point represents a monthly median, and dashed line corresponds to the linear fit for these data, the correlation coefficient is r = 0.61. The correlation algorithm shown in Fig. 5a is used to calculate some missing data in the fmin data sets (e.g. caused by technical reasons), and by this way to restore their continuity.

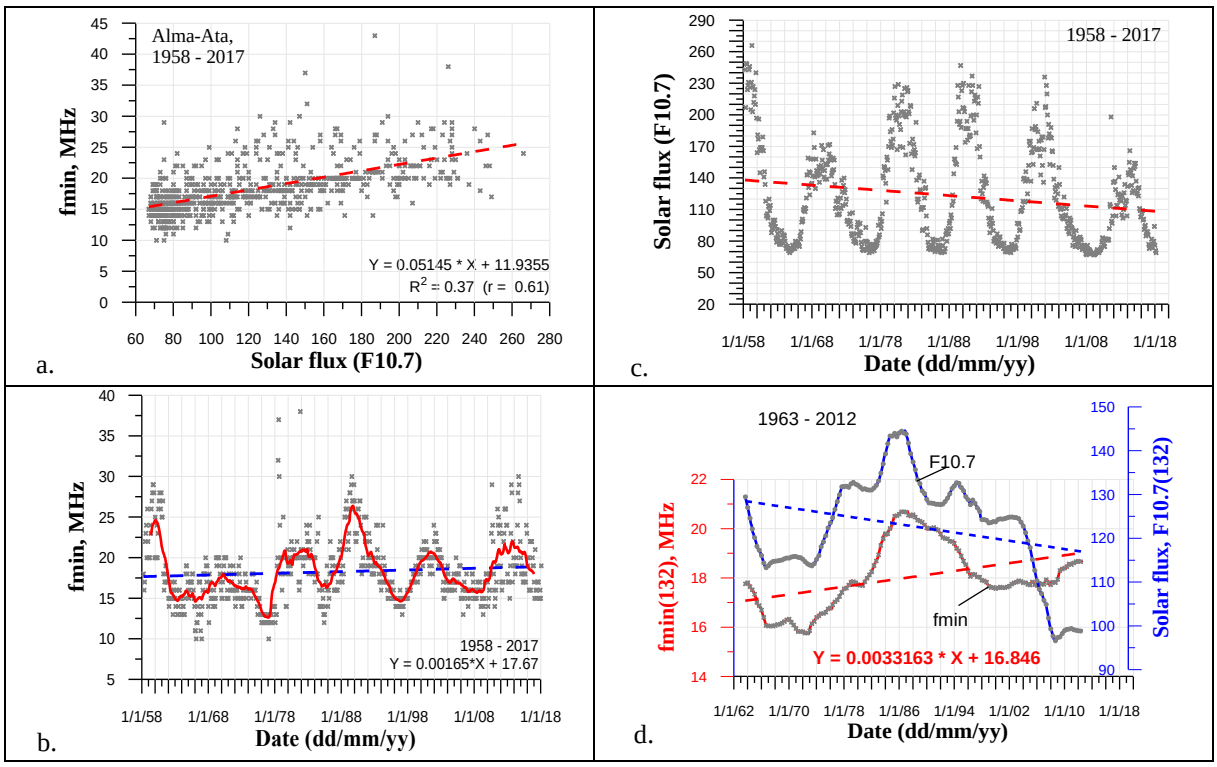

Figure 5. The monthly median near-noon fmin dependence on the solar activity index F10.7 (a) and their long-term variations (b, c). The 132-month smoothed values of fmin and F10.7 (d) where the dashed lines represent their linear trends for the whole measuring interval.

Figure 5b demonstrates the fmin time series in the whole period considered where the clear 11-year periodicity is evident in the fmin variation that is well correlated to that observed in the solar activity (Fig. 5c). In addition we note that, while F10.7 shows a negative time trend for the period in question, the fmin values are experiencing a weak positive trend.

Then, the fmin data sets were smoothed using the 11-year running mean smoothing to suppress effects of the 11-year cycle of the solar activity in the fmin data, and to obtain a picture of long-term variation in them. Figure 5d shows the smoothed fmin and F10.7 variations together with the regression lines (dashed lines), and demonstrates that the long-time course of fmin(132) is similar to those found for F10.7 and foF2 (Figures 1-3) in the event that the periodicity of 34-36 years is also evident in the fmin(132) variation which is found in variations of the F2-layer parameters. However, Figure 5d clear illustrates a stable upward (positive) trend in fmin(132) values in the period 1963-2012 (49 years), opposite in sigh to the trends observed in variations F10.7 and foF2.

There were only few studies of trend in the D-region until the 2019-s. Historical results, which were obtained by using various datasets derived from several different methods of measurements and modeling, were reviewed by Lăstovička and Bremer [42]. It was found that below about 85-90 km all data provided a positive trend in electron densities at fixed heights in qualitative agreement with the cooling and thermal contraction of the mesosphere. Bremer [27] investigated the ionospheric absorption measurements in the LF, MF, and HF ranges at oblique incidence of different distances (distances between transmitter and receiver are from about 170 km to 500 km, and 1710 km), only positive trends were deduced. Note, along with these results our results show the same tendency, the positive trend in the long-term variation of the fmin data. So, we can conclude from the above data analysis that the long-term evolution of fmin demonstrates a clear dependence on solar activity index F10.7, but in contrast to F10.7 the fmin data shows a small positive trend which is statistically significant, although it is not significantly different from zero. It means relatively high sensitivity of the fmin values to the solar activity changes and significant influence of other trend drivers on them that is very possible the impact of anthropogenic factors on the state of the lower ionosphere.

Conclusion.

The F2-layer critical frequency (foF2) and the lowest frequency (fmin) observed at the midlatitude ionospheric station Alma-Ata [43.25ºN, 76.92ºE) in the period 1957-2017 were used to study long-term trends in the upper (F2-layer) and lower (D-region) ionosphere. The geomagnetic (Ap) indexes, the near-noon, near-midnight, daily averaged foF2, and near-noon fmin variations are found to be in strong dependence from the solar activity; all of them show a dominant pattern of variation with a period of ~34-36 years and linear negative trend.

The same order of the trend magnitudes in the foF2 variations are found to be of the same order independently of the fact whether the solar activity effects in the data sets are smoothed or not; the trends are statistically significant and lie within of -0.018 to -0.028, -0.011 to -0.019, -0.0036 to -0. 0093 MHz/year for near-noon, daily averaged and near-midnight values correspondingly. Residual ΔfoF2 values (an example for near-noon hours), where variations

in foF2 related to the solar activity cycles have been removed, show the linear trend of -0.00554 MHz/year. The correlation coefficient between the foF2 and F10.7 long-term variations is very high, up to 0. 99 that permit us to believe that the solar activity can be considered to be the main driver for the long-term variations in the ionospheric F2-region.

The long-term course of fmin is similar to those found in F10.7, Ap, and foF2, i.e. the periodicity of 34-36 years is also evident in the fmin variations. However, in contrast to the F2-layer parameters, the fmin variation clear demonstrates an upward (positive) linear trend that is opposite in sign to the trend found in the F10.7. This means relatively high sensitivity of the fmin values to the solar activity changes and significant influence of other trend drivers on them, one of which is the possible impact of anthropogenic factors on the state of the lower ionosphere.

Acknowledgments

The ionospheric data for the Kazakhstan station Alma-Ata are archived at the Institute of Ionosphere, Kamenskoe Plato, Almaty 050020, Kazakhstan. The monthly mean solar flux F10.7 and geomagnetic index Ap are available at http://www.swpc.noaa.gov/. The Institute of Ionosphere Working Group (GG, AYa, and YuL) was supported by Grant № AP05131261 from Ministry of Education and Science of Kazakhstan.

References

1.R.G., R. E. Dickinson (1989), How will changes in carbon dioxide and methane modify the mean structure of the mesosphere and thermosphere? Geophys. Res. Lett., 16, 1441-1444

2.Rishbeth, H. (1990), A greenhouse effect in the ionosphere? Planet. Space Sci., 38, 945–948.

3.Rishbeth, H., R. G. Roble (1992), Cooling of the upper atmosphere by enhanced greenhouse gases – modelling of the thermospheric and ionospheric effects, Planet. Space Sci., 40, 1011–1026.

4.Mikhailov, A. V. and D. Marin (2000), Geomagnetic control of the foF2 long-term trends, Annales Geophysicae 18, 653-665.

5.Mikhailov, A. V. and D. Marin (2001), An interpretation of the foF2 and hmF2 long-term trends in the framework of the geomagnetic control concept, Annales Geophysicae, 19, 733-748.

6.Danilov, A. D. (2002), The method of determination of the long-term trends in the F2 region independent of geomagnetic activity, Annales Geophysicae, 20, 511–521, doi:10.5194/angeo-20-511-2002.

7.Danilov, A. D. (2003), Long-term trends of foF2 independent of geomagnetic activity. Ann. Geophys., 21, 1167–1176, doi:10.5194/angeo-21-1167-2003.

8.Danilov, A. D. (2008), Long-term trends in the relation between daytime and nighttime values of foF2, Ann. Geophys., 26, 1199-1206.

9.Mikhailov, A. V., D. Marin, T. Yu. Leschinskaya, and M. Herraiz (2002), A revised approach to the foF2 long-term trends analysis, Annales Geophysicae, 20, 1663–1675.

10.Bremer, J. (2004), Investigations of long-term trends in the ionosphere with world-wide ionosonde observations, Advances in Radio Science, 2, 253-258.

11.Yue, X, W. Wan, L. Liu, B. Ning, B. Zhao (2006), Applying artificial neural network to derive long-term foF2 trends in the Asia/Pacific sector from ionosonde observations, J. Geophys. Res. 111, A10303, doi:10.1029/2005JA011577.

12.Mikhailov, A. V. (2006), Ionospheric long-term trends: can the geomagnetic control and the greenhouse hypotheses be reconciled? Annales Geophysicae 24, 2533–2541.

13.Lăstovička, J, X. Yue, W. Wan (2008a), Long-term trends in foF2: their estimating and origin, Ann. Geophys., 26, 593–598.

14.Mielich, J., J. Bremer (2013), Long-term trends in the ionospheric F2 region with different solar activity indices, Ann. Geophys. 31, 291–303.

15.Perrone, L., A. Mikhailov (2016), Geomagnetic control of the midlatitude foF1 and foF2 long-term variations: Recent observations in Europe, J. Geophys. Res. Space Physics, 121, 7183-7192, doi:10.1002/2016JA022715.

16.Danilov, A. D., A. V. Konstantinova (2016a), Trends in the critical frequency foF2 after 2009, Geomagnetism and Aeronomy, 56 (3), 302-310.

17.Danilov, A. D., A. V. Konstantinova (2016b), Long-term changes in the relations between foF2 and hmF2, Geomagnetism and Aeronomy, 56 (5), 577-584.

18.Perrone, L., A. Mikhailov, C. Cesaroni, L. Alfonsi, A. De Santis, M. Pezzopane and C. Scotto (2017), Long-term variations of the upper atmosphere parameters on Rome ionosonde observations and their interpretation, J. Space Weather Space Clim., 7, A21, 11p.

19.Qian, L., S.C. Solomon, R.G. Roble, T.J. Kane (2008), Model simulations of global change in the ionosphere, Geophys. Res. Lett., 35, L07811, 5 p. doi:10.1029/2007GL033156.

20.Mikhailov, A., V. Perrone (2016), Geomagnetic control of the midlatitude foF1 and foF2 long-term variations: Physical interpretation using European observations, J. Geophys. Res. Space Physics, 121, 7193-7203, doi:10.1002/2016JA022716.

21.Solomon, S. C., H.-L. Liu, D. R. Marsh, J. M. Mcinerney, L. Qian, and F. M. Vitt (2018), Whole Atmosphere Simulation of Anthropogenic Climate Change, Geophys. Res. Lett., 45, 1567-1576. https://doi.org/10.1002/2017GL076950.

22.Lăstovička, J. (2002), Long-term changes and trends in the lower ionosphere, Physics and Chemistry of the Earth 27, 497-507.

23.Lăstovička, J, R. A. Akmaev, G. Beig, J. Bremer, J. T. Emmert, C. Jacobi, M. J. Jarvis, G. Nedoluha, Y. I. Portnyagin, T. Ulich (2008b), Emerging pattern of global change in the upper atmosphere and ionosphere, Ann. Geophys., 26, 1255–1268.

24.Lăstovička, J. (2009), Global pattern of trends in the upper atmosphere and ionosphere: Recent progress, J. Atmos. Sol.-Terr. Phys., 71, 1514-1528.

25.Lăstovička, J. (2013), Trends in the upper atmosphere and ionosphere: Recent progress, J. Geophys. Res. Space Physics, 118, 3924-3935, doi:10.1002/jgra.50341.

26.Lăstovička, J. (2017), A review of recent progress in trends in the upper atmosphere, J. Atmos. Sol.-Terr. Phys., 163, 2-13.

27.Bremer, J. (2005), Long-term trends in different ionospheric layers, Radio Science Bulletin, 315, 22-32.

28.Cnossen, I. (2012), Climate Change in the Upper Atmosphere, Greenhouse Gases - Emission, Measurement and Management, Dr Guoxiang Liu (Ed.), ISBN: 978-953-51-0323-3, In Tech, Available from: http://www.intechopen.com/books/greenhouse-gases-emission-measurement-and-management/climatechange-in-the-upper-atmosphere.

29.Danilov, A. D. (2012), Changes in the upper atmosphere and ionosphere over the last decades (Review, in Russian), In: http://vestnik.geospace.ru/issues/iss1/article2.pdf.

30.Danilov, A. D. and A. V. Konstantinova (2015), Comparison of trends in parameters of the F2 layer obtained by various authors, Geomagnetism and Aeronomy, 55(4), 457-466.

31.Laštovička, J., A. V. Mikhailov, T. Ulich, J. Bremer, A.G. Elias, N. Ortiz de Adler, V. Jara, R. Abarca del Rio, A. J. Foppiano, E. Ovalle, A. D. Danilov (2006), Long-term trends in foF2: a comparison of various methods, J. Atmos. Solar. Terr. Phys., 68, 1854–1870.

32.Bremer, J. (2008), Long-term trends in the ionospheric E and F1 regions, Annales Geophysicae, 26, 1189–1197, www.ann-geophys.net/26/1189/2008/.

33.Gordiyenko, G. I., V. V. Vodyannikov, A. F. Yakovets and Yu. G. Litvinov (2014), Earth Planets and Space, 66 (125), 1-6, http://www.earth-planets-space.com/content/66/1/125.

34.Wright, J.W., R.W. Knecht, K. Devies (1956), Mannual on ionospheric vertical soundings for the international geophysical year, Prepared at CRPL National Bureau of Standards Boulder, Colorado, USA, in Russian, Ed. by Mednikova N.V., and Shapiro B.S. Moscow-1957, 224 p.

35.Lauter, E. A., G. Entzian (1982), Vinter anomaly 1980/81 as an example of stratomesospheric coupling, Phys. Solariterr., 18, 83-90.

36.Kokourov, V. D. (2003), Minimum frequency of reflections as a climatic characteristic of the upper atmosphere, Geomagnetism and Aeronomy, 43(2), 274-276, in Russian.

37.Clúa de Gonzalez A. L, W. D Gonzalez, S. L. G. Dutra, B. T Tsurutani (1993), Periodic variation in the geomagnetic activity: a study based on the Ap index, J Geophys. Res., 98, 9215.

38.Echer, E., N. R. Rigozo, D. J. R. Nordemann, and L. E. A. Vieira (2004), Prediction of solar activity on the basis of spectral characteristics of sunspot number, Annales Geophysicae, 22, 2239-2243.

39.Prabhakaran Nayar, S. R. (2006), Periodicities in solar activity and their signature in the terrestrial environment, IL WS WORKSHOP, GOA, February 19-24, 9 p.

40.Henry, A. J. (1927), Brückner cycle of climatic oscillations in the united states, Annals of the Association of American Geographers, 17(2), 60-71.

41.Raspopov, O. M., O. I. Shumilov, E. A. Kasatkina, E. Turunen, M. Lindholm (2000), 35-year climatic Bruckner cycle-solar control of climate variability, Proc. 1st Solar and Space Weather Euroconference "The Solar Cycle and Terrestrial Climate", Santa Cruz de Tenerife, Tenerife, Spain, 25-29 September 2000 (ESA SP-463, December 2000).

42.Lăstovička, J. and Bremer J. (2004), An overview of long-term trends in the lower ionosphere below 120 km, Surv. Geophys., 25, 69-99.

DETERMINATION OF LANTHANIDES AND 3D METALS IN ENDOMETALLOFULLERENES WATER SOLUTIONS BY X-RAY FLUORESCENCE SPECTROMETRY

DOI: 10.31618/ESU.2413-9335.2019.4.65.271

Zinovyev V. G.,.Lebedev V.T,
Mitropolsky I. A.,. Shulyak G. I,
Sushkov P. A.,. Tyukavina T. M,
Okunev I. S.,. Ershov K.V, Balin D.V.
Petersburg Nuclear Physics Institute named by B.P.Konstantinov of NRC «Kurchatov Institute»

ABSTRACT

An XRF method was developed for determination of Fe, Co, Ni, Mn, Mo, Sc, Gd, Tb and Pr in endo-fullerenes. The synthesis of endofullerenes was carried out in a direct current arc in helium medium. The content of endofullerenes of 3d metals in the soot was increased by introduction of two graphite electrodes made of phthalocyanine of 3d metals and lanthanides into the arc. The extraction of endofullerenes of 3d metals and lanthanides by N,N dimethylformamide in presence of 0.2% vol. hydrazine hydrate has increased the yield of endo-fullerenes of lanthanides and 3d metals by 2–3 times. The hydroxylation of endofullerenes of 3d metals obtained from the fullerene dimethylformamide extract was carried out with concentrated H_2O_2. It was established that the yield of the water-soluble endofullerene product depends on concentration of H_2O_2 in the solution and duration of the process.

Keywords: Fullerenes, X-ray fluorescence analysis, extraction

The endofullerenes of 3d-metals and lanthanides can be used for medical purposes: for NMR tomography and for magnetically controlled delivery of drugs to the diseased organ. The endofullerenes are used in drugs for treatment of neurodegenerative diseases such as Alzheimer disease, Parkinsonism and others. Usually, endofullerenes are produced by arc or